

## Polypeptides | Hot Paper |

## A Pure Polyproline Type I-like Peptoid Helix by Metal Coordination

Lieby Zborovsky, Alisa Smolyakova, Maria Baskin, and Galia Maayan<sup>\*[a]</sup>

**Abstract:** Peptoids, N-substituted glycine oligomers, are an important class of foldamers that can adopt polyproline-type helices (PP-I and PP-II), given that the majority of their sequence consists of chiral, bulky side chains. Herein a new approach for the stabilization of a pure PP-I-like peptoid helix through metal coordination is introduced. A systematic spectroscopic study was performed on a series of peptoid heptamers bearing two 8-hydroxyquinoline ligands at fixed positions, and a mixture of chiral benzyl and alkyl substitu-

ents in varied positions along the peptoid backbone. When the benzyl groups are located at the 3rd and 4th positions, the peptoid (**7P6**) gives upon Cu<sup>2+</sup> binding a circular dichroism (CD) signal similar to that of a PP-I helix. Exciton couplet CD spectroscopy and EPR spectroscopy, as well as modifications to the length of **7P6** and derivatization through acetylation provided insights into the unique folding of **7P6** upon Cu binding, showing that it is led by two competing driving forces, namely coordination geometry and sequence.

## Introduction

Folding of natural biopolymers is an important event, in which specific arrangements of various functional groups lead to the generation of reactive centers. The established relationship between the structure and function of natural biopolymers has inspired the design of "foldamers": biomimetic oligomers that fold into three-dimensional structures in solution.<sup>[1]</sup> Peptoids, oligomers of N-substituted glycine, are an important class of peptide mimics capable of forming well-defined secondary structures,<sup>[2]</sup> and performing various biological functions.<sup>[3]</sup> Peptoid oligomers can be synthesized efficiently by solid-phase methods,<sup>[4]</sup> granting the facile utilization of a large scope of side chains, thus allowing the introduction of different functional groups.<sup>[2]</sup> One example is the incorporation of metal binding ligands aiming to form metallopeptoids.<sup>[5–7]</sup> This has led to peptoid chelators, which were utilized for the synthesis of metal-containing biomimetic scaffolds with intriguing properties, and some were applied in selective recognition and catalysis.<sup>[5–7]</sup>

Although peptoids are incapable of forming hydrogen-bonded networks along the backbone, many peptoid sequences exhibit a remarkable tendency for folding.<sup>[2]</sup> It was previously demonstrated that peptoids, which at least two thirds of their backbones consist of bulky N- $\alpha$ -chiral residues, are capable of adopting polyproline-like helical secondary structures owing to local steric and stereo-electronic interactions.<sup>[8]</sup> In

contrast to polyproline peptides that are composed of either *cis* or *trans* amide bonds, peptoid monomers can favor both *cis* and *trans* orientation of the amide bond. This can be easily determined using circular dichroism (CD) spectroscopy, which is a key tool for describing the secondary structure of peptoids. Typical CD spectra of peptoids having only  $\alpha$ -methyl-benzyl side chains ( $\alpha$ -methyl-benzyl peptoids), for example, measured in organic solvents such as methanol and acetonitrile, exhibit double minima near 200 and 220 nm owing to the presence of both the *trans*- and *cis*-amide bonds, respectively.<sup>[9]</sup> This is because  $\alpha$ -methyl-benzyl peptoids, although generally adopting PP-I type helices with a pitch of three residues per turn,<sup>[9,10]</sup> contain a minor population of conformers consisting of one or more *trans*-amide bonds.<sup>[9]</sup> As a consequence, controlling peptoid conformation is nontrivial, and thus, a major objective is to produce all-*cis* PP-I-like peptoid helices as a basis for further applications in biology,<sup>[3]</sup> asymmetric catalysis,<sup>[11]</sup> selective recognition<sup>[5*i,j,m*]</sup> and more.<sup>[12]</sup> Efforts toward this goal focus on the development of chiral, bulky side chains that could grant a considerable energetic preference for the *cis* amide bond conformation.<sup>[13]</sup> These efforts resulted in the four best *cis*-directing side chains reported, namely triazole-based side chains,<sup>[14]</sup> (*S*)-*N*-(1-naphthylethyl)glycine (*Ns1 npe*),<sup>[15]</sup> *tert*-butyl (*t*-Bu) and (*S*)-*N*-(1-*tert*-butylethyl)glycine (*Ns1 tbe*).<sup>[16]</sup> Each side chain was used for the construction of peptoid homo-oligomers with various lengths exhibiting all-*cis* PP-I-type helices, as demonstrated by high-resolution structural studies including X-ray crystallography and NMR spectroscopy, as well as from CD spectroscopy. Notably, the CD spectra of oligomers with six-to-nine *Ns1 tbe* monomers represent an exceptional example in which their CD spectra resembles that of a PP-I-type peptide helix. Although these structures are quite remarkable, they are also unique, drastically limiting the sequence and functional diversity of all-*cis* PP-I-type peptoid helices, which presently can only

[a] Dr. L. Zborovsky, A. Smolyakova, M. Baskin, Prof. G. Maayan  
Schulich Faculty of Chemistry  
Technion–Israel Institute of Technology  
Haifa, 32000 (Israel)  
E-mail: gm92@technion.ac.il

Supporting information of this article can be found under:  
<https://doi.org/10.1002/chem.201704497>.

be generated from four specific side chains out of the many that exist. Therefore, an entirely different approach toward the formation of pure PP-I peptoid helices should be considered to increase peptoid helices diversity, and may be developed by the use of metal coordination, which proved efficient in the case of peptide helix stabilization.<sup>[17]</sup> Moreover, understanding the relationship between peptoid folding and metal binding should shed some light on the relationship between peptoid structure and function in general, expanding the limited knowledge in this field, thus limiting the applications of metallopeptoids.

Earlier work by Maayan et al. demonstrated that the incorporation of two 8-hydroxyquinoline (HQ) groups within the backbone of a helical peptoid, with chiral-bulky (*S*)-(-)-1- $\alpha$ -methylphenylethylamine (*N*spe) substituents (**H<sub>2</sub>6**, Figure 1 a, top) can be utilized for intramolecular binding of copper and cobalt metal ions.<sup>[6]</sup> Interestingly, metal binding to the HQ groups, which were located at 2nd and 5th positions (*i* and *i*+3), affected the peptoid secondary structure and increased the peptoid helicity as was evidenced by the enhanced intensity of

the CD double-minima signal at about 200 and 220 nm (Figure 1 a, bottom).<sup>[6]</sup> Inspired by this report, we recently attempted to induce secondary structure by metal binding to a completely unfolded peptoid.<sup>[7]</sup> We expected that metal binding would tighten the peptoid backbone resulting in a more helical structure. Thus, a water-soluble heptameric peptoid (**7mer-HQ2**, Figure 1 b, top), having two HQ groups located at the 2nd and 5th positions, and five chiral, non-bulky *N*-*S*-methoxypropyl (*N*smp) groups was synthesized.<sup>[7]</sup> *N*smp groups are not bulky enough to induce secondary structure. However, the chirality of the *N*smp groups allows for analysis of the secondary structure by CD. Disappointingly, no helix formation was observed upon binding of copper or cobalt ions, as was ascertained by analyzing the CD spectra of the free **7mer-HQ2** (Figure 1 b, bottom, blue line) and its copper and cobalt complexes (Figure 1 b, bottom, red and green lines, respectively) in the range of 190–230 nm, all of which suggest completely disordered structures.<sup>[7]</sup> These results imply that a helical structure cannot be induced solely by metal coordination. Overall these studies demonstrate that metal binding can increase the helicity of *N*spe peptoids while maintaining the mixed population of PP-I- and PP-II-like helices, on one hand, and cannot affect the helicity of disordered peptoids on the other hand. Accordingly, we attempted the formation a pure PP-I-like peptoid helix upon metal binding, which will give rise to a CD spectrum that resembles that of a PP-I peptide helix. To this end, we decided to investigate coordination of metal ions to peptoids that exhibit low-intensity HQ double minima in CD spectra, and try to increase the population of *cis*-amide bonds while decreasing the *trans*-amide bond population.

Herein we report the design, synthesis, and characterization of a series of peptoid oligomers containing a combination of chiral-bulky and chiral-non-bulky substituents. We study the effect of metal binding on the formation of peptoid helical structures and demonstrate the ability to increase the population of the *cis*-amide bond conformers by metal binding, as evident from CD spectroscopy. We show that the largest effect of metal binding is in the case of a “bulky-core” peptoid having two *N*spe groups at the 3rd and 4th positions that give rise to a low-intensity double minima CD spectrum. Upon Cu<sup>2+</sup> coordination, the CD spectrum drastically changes and resembles a typical CD spectrum of a PP-I helical peptide and the CD spectra of the all-*cis* *N*s1 npe- and *N*s1 tbe-based PP-I peptoid helices.

## Results and Discussion

### Design and synthesis of peptoid oligomers

Eight peptoid oligomers, **7P1–7P8** (Figure 1 c) were synthesized, using 8-hydroxy-2-quinolinemethylamine (HQ), (*S*)-(-)-1- $\alpha$ -methylphenylethylamine (*N*spe) and (*S*)-(+)-1-methoxy-2-propylamine (*N*smp) as synthons, employing “submonomer” protocols.<sup>[18]</sup> HQ is a strong chelator for divalent metal ions such as Co<sup>2+</sup>, Cu<sup>2+</sup>, and Zn<sup>2+</sup>.<sup>[19]</sup> All peptoids consist of seven monomers and bear two HQ groups incorporated at the 2nd and 5th positions. These positions were chosen in accordance

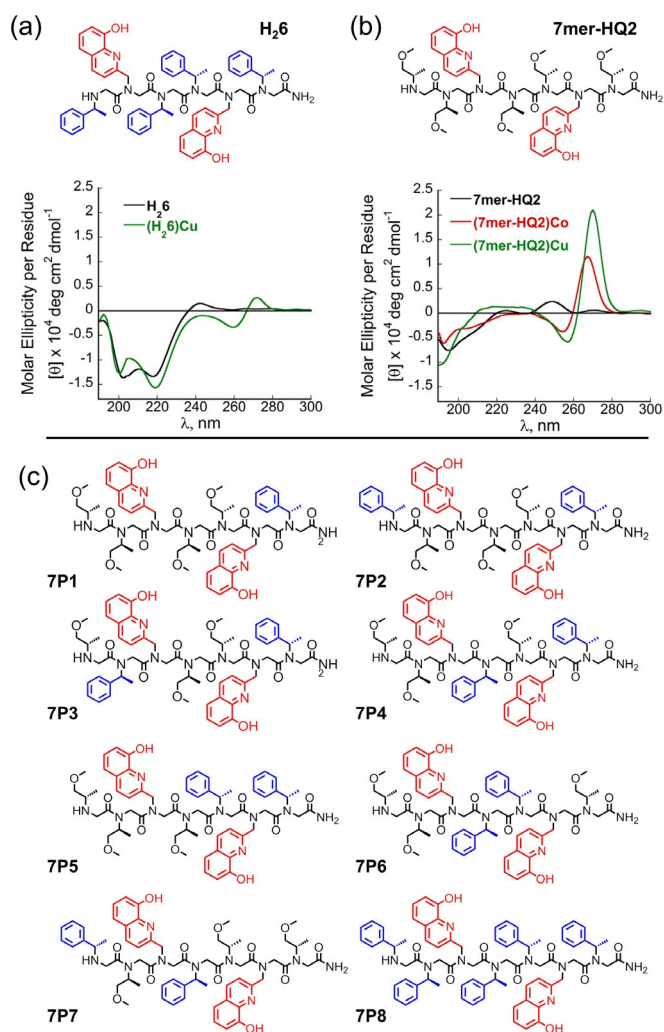


**Figure 1.** a) Chemical sequence of **H<sub>2</sub>6** and CD spectra of **H<sub>2</sub>6** and its Cu<sup>2+</sup> complex.<sup>[6]</sup> b) Chemical sequence of **7mer-HQ2** and CD spectra **7mer-HQ2** and its metal complexes.<sup>[7]</sup> c) Chemical sequences of oligomers **7P1–7P8**.

with the three residues per turn structure of the peptoid helix.<sup>[6]</sup> Placing the HQ groups in these positions was expected to provide a more efficient metal binding and a tighter structure.<sup>[6]</sup> It is known that the driving force for folding of peptoids is the incorporation of at least 66% chiral-bulky side chains out of all the substituents within the sequence.<sup>[2]</sup> Our strategy was to reduce the peptoid helicity by using less than 66% of chiral-bulky substituents and to attempt increasing of its helicity by metal coordination. Thus, peptoid **7P1** was synthesized with one *Nspe* group at the 1st position (14% of the monomers) and **7P2** was synthesized with two *Nspe* groups in the 1st and 7th positions (28% of the monomers). A key parameter that determines the helicity of the peptoid backbone is the position of the *Nspe* groups along the peptoid chain.<sup>[20]</sup> Thus, oligomers **7P3–7P7** were designed to have alterations in the sequence of **7P2** such that the two *Nspe* groups are shifted to different positions along the peptoid chain. As an example of a fully helical peptoid that can serve as a reference point, **7P8** with five *Nspe* groups was synthesized. All peptoids were synthesized on solid support followed by their cleavage at the end of the synthesis and purification by HPLC (>95%). The molecular weights measured by electrospray mass spectrometry (ESI-MS) were consistent with the expected masses (see the Supporting Information).

### UV/Vis analysis

The metal-free peptoids exhibited absorption bands near  $\lambda = 245$  nm and 306 nm in 80% aqueous methanol solution. Upon addition of metal acetate [ $M(\text{Ac})_2$ ;  $M = \text{Co}, \text{Cu}, \text{Zn}$ ], binding of  $M^{2+}$  produced new absorption bands at  $\lambda = 265, 383$  nm for  $\text{Zn}^{2+}$  and  $\text{Co}^{2+}$  and  $\lambda = 265, 390$  nm for  $\text{Cu}^{2+}$ . Representative plots are depicted in Figure 2, showing the absorbance band of the free peptoids in red and the absorbance band of their  $\text{Cu}^{2+}$  complexes in blue (for other plots see the Supporting Information). Titration experiments with  $M(\text{Ac})_2$  using UV/Vis spectroscopy confirmed that the complexes are formed in 1:1 metal-to-peptoid ratio (Figure 2, inset). This ratio suggests that the metal is bound in an intramolecular mode to two HQ ligands, and this was further supported by ESI-MS (see the Supporting Information).

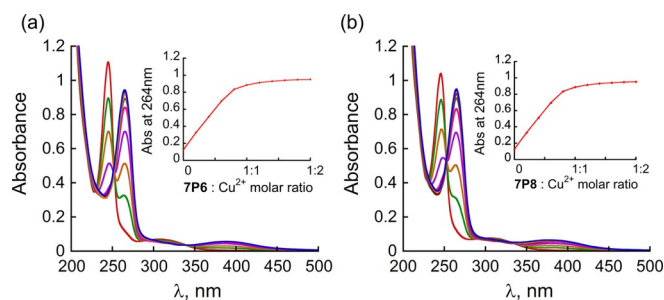


**Figure 2.** UV titrations of a) 16.6  $\mu\text{M}$  **7P6** and b) 16.6  $\mu\text{M}$  **7P8** with  $\text{Cu}(\text{Ac})_2$  in 80% aqueous MeOH.

### CD analysis

The CD spectra of all peptoids were measured in 80% aqueous methanol. Peptoid **7mer-HQ2**, with no bulky-chiral groups, shows no double minima in the CD spectrum indicating its disordered secondary structure (Figure 1a).<sup>[7]</sup> Aiming to explore whether we can initiate helicity within this peptoid, we replaced the *Nsmp* group in the first position by an *Nspe* group, because this position of the peptoid sequence was shown to determine the peptoid helicity according to the “sergeant–soldiers” effect.<sup>[20]</sup> Indeed, the CD spectra of **7P1** with only one *Nspe* group at the 1st position demonstrates low intensity double minima consistent with the initiation of a helical structure formation (Figure 3a). Binding of either  $\text{Co}^{2+}$  or  $\text{Zn}^{2+}$  did not have a significant effect on the CD spectrum of the unbound peptoid, whereas the binding of  $\text{Cu}^{2+}$  results in a decrease in the intensity of the spectrum. The latter can be attributed to structural changes within the peptoid, enforced by the coordination geometry of the copper complex. In attempts to further explore this, we replaced one more *Nsmp* group by an *Nspe* group. Thus, we synthesized oligomers **7P2–7P5**, which have an *Nspe* group in the 1st position but differ in the position of the other *Nspe* group that is located at the 7th, 6th, 4th, and 3rd position respectively. From examining the CD spectra of these oligomers, we can see that all of them have

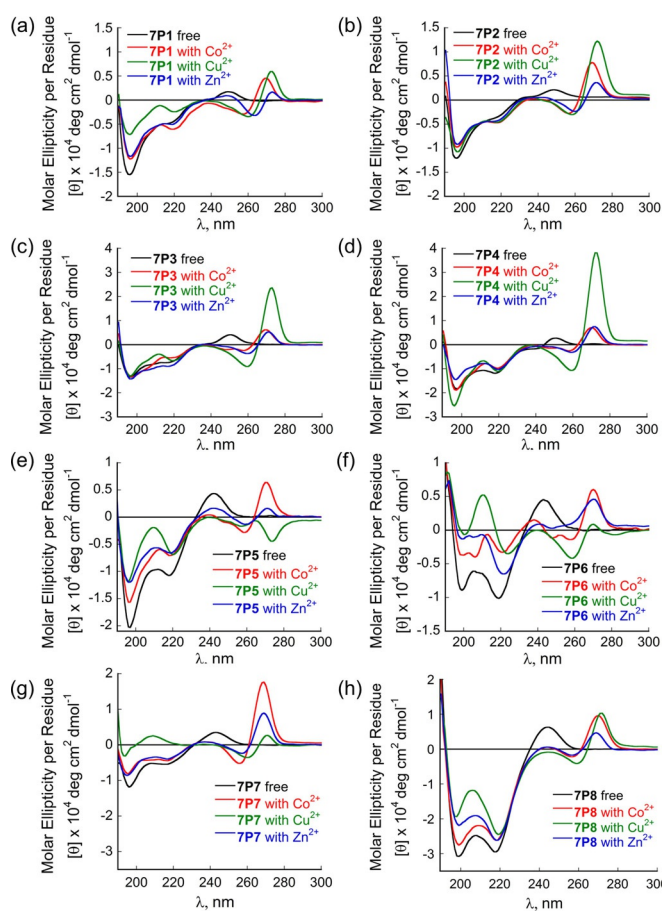


**Figure 3.** CD spectra of oligomers **7P1–7P8** and their  $\text{Co}^{2+}$ ,  $\text{Cu}^{2+}$ , and  $\text{Zn}^{2+}$  complexes (100  $\mu\text{M}$  in 80% aqueous methanol).

some extent of helicity that can be attributed to the *Nspe* group at the determining 1st position.<sup>[20]</sup> However, the intensity of the double minima depends strongly on the position of the second *Nspe* group. Thus, oligomers **7P2** (Figure 3 b) and **7P3** (Figure 3 c), with the second *Nspe* group at the 7th and 6th positions respectively, exhibit low intensity, mostly disordered CD spectra, while oligomers **7P4** (second *Nspe* group at the 4th position, Figure 3 d) and **7P5** (second *Nspe* group at the 3rd position, Figure 3 e) show a higher intensity signal compared with that of **7P2** and **7P3**, with a more pronounced double minima around 200 and 220 nm, indicating a more helical structure. Shifting the *Nspe* group of **7P2** from the 1st to the 4th position, to give **7P7**, results in an expected decrease of the CD intensity and a nearly complete loss of the double minima (Figure 3 g). Oligomer **7P6** with the two *Nspe* groups located at the 3rd and 4th positions, between the two HQ groups, showed pronounced double minima at 200 and 220 nm (Figure 3 f). The intensity of the double minima, especially the peak at 220 nm, which corresponds to the *cis* amide bond, indicates a more ordered helical structure compared with **7P1–7P5**. This result is surprising because **7P6** does not have a bulky-chiral group situated at the crucial 1st position. This observation can probably be attributed to the formation of a bulky-core segment in the middle of the peptoid sequence that promotes the formation of a helical secondary structure. **7P8** (Figure 3 h) substituted by five *Nspe* groups, which was synthesized as a control peptoid for comparison with the other *Nspe* peptoids, exhibited, as expected, the most ordered structure as can be seen from the relatively high intensity CD signal with distinct double minima at 200 and 220 nm. In addition to the CD signals in the range of 190–230 nm, all metal-free peptoids exhibit a CD peak at about 250 nm. This peak corresponds to the absorption of the HQ ligand as was shown by UV measurements (Figure 2). As the HQ ligand is achiral, its appearance in the CD spectra indicates chiral induction from the peptoid backbone.

In all cases except for **7P6**, addition of  $Zn^{2+}$  or  $Co^{2+}$  has only a small effect on the CD spectrum of the peptoids in the near-UV region. Binding of  $Cu^{2+}$  results in the decrease of CD intensity for **7P5**, **7P7**, and **7P8** and does not change the CD spectrum of **7P2**, **7P3**, and **7P4**. As discussed above, the CD spectra of the free peptoids **7P5**, **7P7**, and **7P8** exhibit some degree of helicity as indicated by the typical double minima signal, whereas **7P2**, **7P3**, and **7P4** do not. Notably, the coordination geometry of the formed copper complexes enforces structural changes (as was observed in the case of **7P1**) only within the peptoids that have some secondary structure prior to  $Cu^{2+}$  binding. Specifically, in **7P4**, which exhibits low-intensity double minima, an increase in the intensity of the band at 200 nm is observed compared to the band at 220 nm that does not change at all. This observation suggests an increase in the population of the *trans*-amide bond conformers of this peptoid in solution upon  $Cu^{2+}$  binding, and an overall decrease in the stability of its PP-I helical structure. On the other hand, in **7P8**, with the most intense double minima, a more pronounced decrease in the intensity of the band at 200 nm is observed compared to the band at 220 nm, suggesting a de-

crease in the population of the *trans*-amide bond conformers of this peptoid in solution and an overall increase in the stability of its PP-I helical structure. The latter observation is further demonstrated by oligomer **7P6**, which shows the largest effect of metal binding. Coordination of  $Co^{2+}$  results in a significant decrease in the CD intensity of both minima, suggesting the destruction of the secondary structure, probably attributable to geometry coordination considerations (Figure 3 f, red line). The binding of  $Zn^{2+}$  resulted in a significant decrease in intensity only in the band at about 200 nm, which corresponds to the *trans* amide bond, suggesting a change in the structure of the peptoid, not its destruction (Figure 4 F, blue line). Surpris-

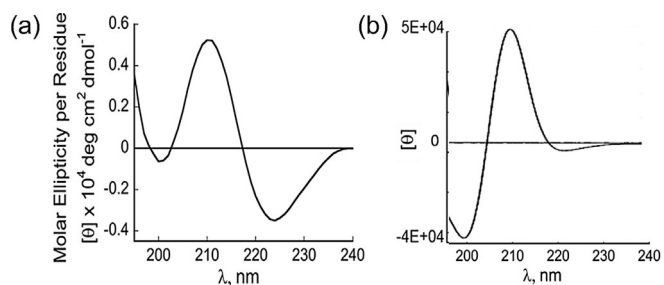


**Figure 4.** a) CD spectrum at near-UV of **7P6Cu** (100  $\mu$ M in 80% aqueous methanol). b) Near-UV CD spectrum of PP-I peptide helix.<sup>[21]</sup>

ingly, coordination of  $Cu^{2+}$ , results in a CD signal completely different from that of the free peptoid, exhibiting minima at 200 and 226 nm and a maximum at 212 nm [Figures 3 f, (green line) and 4 a]. These spectra closely resemble that of a PP-I peptide helix<sup>[21]</sup> (Figure 4 b), as can be observed from the comparison of the two spectra in Figure 4, and the CD spectra of the all-*cis* *Ns1npe* and *Ns1tbe* based PP-I peptoid helices. Based on the experimental CD spectrum of **7P6Cu**, we propose that coordination of copper ions to **7P6** results in the formation of a pure PP-I-like helical structure. We assume that the driving force for the formation of this exceptionally ordered helix is the initial secondary structure of **7P6** as implied from the low intensity double minima observed in its CD spectra combined with the coordination geometry of its Cu complex. All-*cis* PP-I-like peptoid helices were previously observed for bulky aliphatic peptoids<sup>[16,22]</sup> or for chiral bulky substituted peptoids.<sup>[15]</sup> Herein, we demonstrate the possibility of achieving a pure PP-I helical structure for mixed aliphatic–aromatic substituted oligomers.

Binding of  $Zn^{2+}$ ,  $Co^{2+}$ , or  $Cu^{2+}$  ions to oligomers **7P1–7P8**, results in the appearance of exciton couplet peaks in the far UV region, located between 240 and 280 nm, and represented by two coupled absorption bands with opposite signs, known to be brought about by the interaction between two chromophores present in the same backbone.<sup>[23]</sup> It was previously demonstrated both by computational and empirical methods that the intensity and wavelength of the exciton couplets depend on the dihedral angle between the two chromophores.<sup>[23]</sup> As the angle between the chromophores increases, the CD magnitude decreases and slightly shifts toward the UV region.<sup>[23]</sup> In this work, the two chromophores correspond to

the two HQ side chains; hence, the angle between these ligands is correlated to the coordination geometry of the metal complex formed. As can be seen in the CD spectra, there is a difference in the intensity of the exciton couplet for complexes of the same peptoid with different metal ions (Figure 3). We assign these differences to the dissimilarity in coordination geometry of the HQ ligands with each metal ion. Moreover, when comparing the exciton couplet peaks of different oligomers with the same metal ion, for example  $\text{Cu}^{2+}$ , differences in intensities are observed (Figure 5a). Thus, peptoids with more

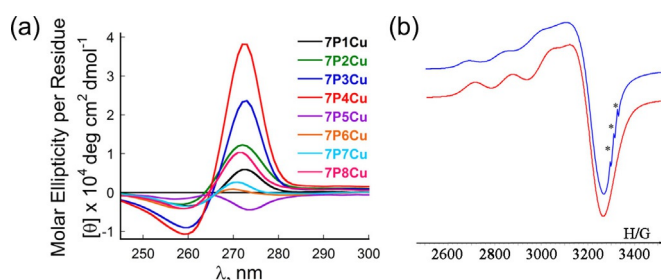


**Figure 5.** a) Far-UV CD spectra of peptoid copper complexes **7P1Cu–7P8Cu** (100  $\mu\text{M}$  in 80% aqueous methanol). b) Room temperature X-band EPR spectra of peptoid oligomer copper complex **7P6Cu** in the solid state (blue line) and the corresponding simulated spectrum (red line). \* = TEMPO reference;  $g = 2.0058$ .

ordered secondary structures for example **7P5**, **7P6**, and **7P8**, exhibit the lowest intensities of the exciton couplet peak, indicating larger dihedral angles between the HQ chromophores. This increase in the dihedral angles, which ultimately leads to a distortion from the preferred coordination geometry of the metal center, can be attributed to the larger steric hindrance that is obtained for the more ordered peptoid structures.<sup>[7]</sup>  $(\text{HQ})_2\text{Cu}$ , for example, is known to adopt the square planar geometry,<sup>[24]</sup> but when this complex is incorporated within a helical peptoid, the peptoid scaffold enforces an unusual coordination environment, leading to the formation of a pseudo-tetrahedral metal complex.<sup>[6]</sup>

### EPR analysis

To obtain more information about the structure of the copper complexes and establish our hypothesis regarding the relationship between the peptoid helicity and coordination geometry of the metal centers, we conducted EPR measurements to all the Cu-peptoids.  $\text{Cu}^{2+}$  complexes have a  $3d^9$  electronic configuration and so are paramagnetic with an electronic spin  $S = 1/2$ , allowing the measurement of their electron paramagnetic resonance (EPR) spectra. EPR measurements can not only confirm the presence of  $\text{Cu}^{2+}$  in the compound but also give insight into the geometry of the formed complex. It was previously suggested that the quotient  $\frac{g_{\perp}}{g_{\parallel}}$  (cm) is a reliable parameter for determining coordination geometry of tetra-coordinated Cu(II) complexes. It ranges between 105–135 for square-planar structures and indicates tetrahedral distortion when higher than 135.<sup>[25]</sup> For  $(\text{HQ})_2\text{Cu}$  the experimental value of the quotient is

134, consistent with a square-planar geometry.<sup>[26]</sup> For **7mer-HQ2** the experimental quotient value was 137, indicating a slight distortion of planarity assigned to the effect of the peptoid backbone on the geometry of the complex.<sup>[6]</sup> In analogy with  $(\text{HQ})_2\text{Cu}$  and **7mer-HQ2**, oligomers **7P1–7P8** are anticipated to form tetragonal complexes when bound to  $\text{Cu}^{2+}$ . The quotient value for these complexes is expected to be higher than 135, as a result of a distortion from square-planar geometry attributed to the peptoid backbone. Thus, the X-band EPR spectra of solid, powdered samples of  $(\text{L})\text{Cu}(\text{PF}_6)$  ( $\text{L} = \mathbf{7P1-7P8}$ ) were recorded at room temperature (a representative spectrum of **7P6Cu** appears in Figure 5b). The EPR signals clearly indicated the presence of a  $\text{Cu}^{2+}$  and the Hamiltonian parameters obtained from their spectra are summarized in Table 1.

Table 1. Hamiltonian parameters of copper complexes $\text{LCu}$ ( $\text{L} = \mathbf{7P1-7P8}$ ). <sup>[a]</sup>				
Complex	$g_{\parallel}$	$g_{\perp}$	$A_{\parallel} \times 10^{-4}$ [ $\text{cm}^{-1}$ ]	$\frac{g_{\perp}}{g_{\parallel}}$ [cm]
$(\text{HQ})_2\text{Cu}$ <sup>[b]</sup>	2.172	2.042	162.0	134
<b>7P1Cu</b>	2.230	2.071	164.5	136
<b>7P2Cu</b>	2.220	2.067	162.7	136
<b>7P3Cu</b>	2.235	2.067	165.9	135
<b>7P4Cu</b>	2.230	2.063	164.5	136
<b>7P5Cu</b>	2.220	2.063	164.8	135
<b>7P6Cu</b>	2.250	2.065	162.8	138
<b>7P7Cu</b>	2.206	2.065	163.3	135
<b>7P8Cu</b>	2.560	2.066	164.7	155

[a] All measurements were performed in the solid state at RT with TEMPO as a reference ( $g = 2.0058$ ). [b] Ref. [26].

The experimental values of the quotient  $\frac{g_{\perp}}{g_{\parallel}}$  (cm) derived from our EPR measurements are about 135–136 for the complexes **7P1Cu–7P5Cu** and **7P7Cu**, indicating a very slight distortion from square-planar geometry. The quotient of **7P6Cu** is 138, implying that it is more distorted toward a tetrahedral geometry. For the helical peptoid complex **7P8Cu** the quotient value is 155. This value corresponds to a tetrahedral geometry of the complex. These results are in line with the assumption that the structure of the peptoid backbone affects the geometry of the formed complex. Thus, a more helical peptoid results in an increased steric bulk around the metal center causing the distortion of the square planar structure. These results correlate well with the CD measurements (Figure 3) that show that the copper complexes **7P6** and **7P8** exhibit a more-ordered helical structure than for complexes **7P1–7P5** and **7P7**.

### Variable temperature CD measurements

To test the thermal stability of the obtained pure PP-I-like structure, we performed CD measurements on both **7P6Cu** and **7P6Cu** complexes at temperatures ranging from 5–60  $^{\circ}\text{C}$  (see the Supporting Information). The CD intensity of free peptoid **7P6** is decreased with increasing temperature, indicating that the overall population of the ordered peptoid in solution is decreased. However, for the copper complex **7P6Cu** only a very slight decrease of the CD intensity at temperatures above

30 °C is observed. This implies that formation of the copper complex **7P6Cu** has an overall stabilizing effect on the peptoid secondary structure, which leads to a higher thermal stability of **7P6Cu** in comparison with the free **7P6**. The positive peak of the exciton couplet, near 275 nm also increases with raising the temperature. As the increase in exciton couplet correlates with the decrease in dihedral angle between the two HQ chromophores,<sup>[23]</sup> we can assume that increasing temperature results in a change in the coordination geometry about the metal center.

### Understanding the factors that contribute to the unique structure of **7P6Cu**

Aiming to understand the role of the bulky-core motif in the formation of the PP-I secondary structure in **7P6**, we synthesized the bulky-core fragment (peptoid tetramer **4P6**, Figure 6)

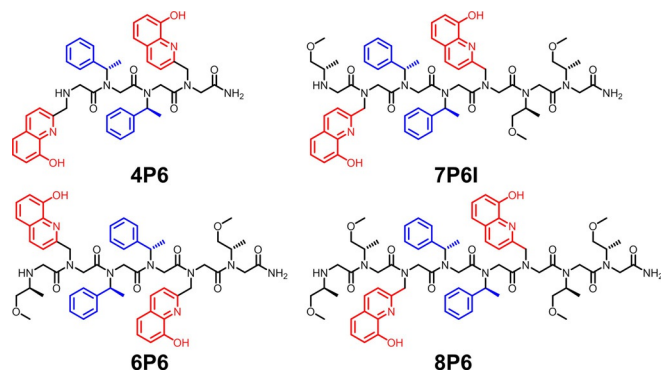


Figure 6. Chemical sequences of oligomers **4P6**, **6P6**, **7P6I**, and **8P6**.

with HQ groups at the 1st and 4th positions and *N*spe groups at the 2nd and 3rd positions. The CD spectra of **4P6** before and after  $\text{Cu}^{2+}$  addition were recorded. Although free **4P6** gives a CD spectrum similar to double minima typical for *N*spe peptoids (see the Supporting Information), addition of copper leads to a decrease in the CD intensity and the band about 220 nm becomes predominant (Figure 7a, black line). This spectrum, however, does not resemble that of a PP-I helix. Thus, the bulky-core by itself is not the only requirement for the formation of a pure PP-I-like peptoid helix upon copper binding, probably because the overall peptoid sequence is too short.<sup>[15]</sup> Consequently, we synthesized three more peptoids, namely **6P6**, **7P6I**, and **8P6** (Figure 6), all containing the bulky-core motif, and measured their CD spectra before and after  $\text{Cu}^{2+}$  addition. Oligomer **6P6** is a symmetrical hexamer with an *N*smp group at the first and last positions. **7P6I** is a derivative of **7P6** with two *N*smp groups near the N-terminus and one *N*smp group near the C-terminus. Aiming to probe the effect of the longer *N*smp tail near the C-terminus, we extended **7P6I** by one *N*smp monomer to give **8P6**, a symmetrical octamer with two *N*smp groups before and after the bulky-core fragment.

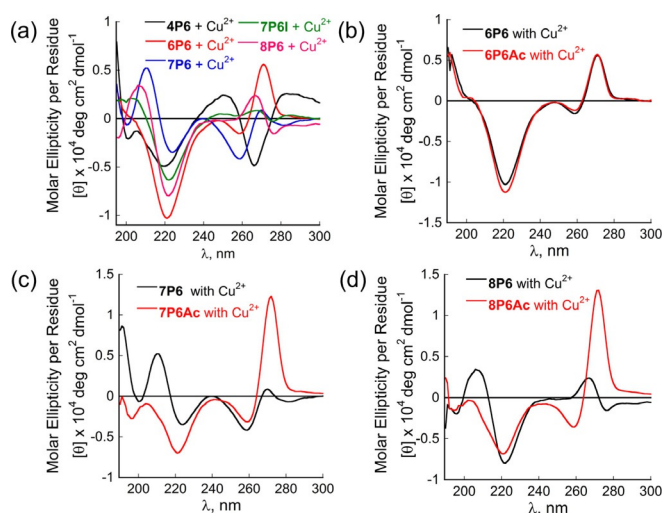


Figure 7. CD spectra of (100 μM in 80% aqueous methanol): a)  $\text{Cu}^{2+}$  complexes of **4P6**, **6P6**, **7P6**, **7P6I**, and **8P6**. b)  $\text{Cu}^{2+}$  complexes of **6P6** and **6P6Ac**. c)  $\text{Cu}^{2+}$  complexes of **7P6** and **7P6Ac**. d)  $\text{Cu}^{2+}$  complexes of **8P6** and **8P6Ac**.

The CD spectra of these three peptoids exhibited the typical double minima of *N*spe peptoids, only with an intensity of about a third compared to this of **7P8** (Figure S80b–d, black lines). Addition of  $\text{Cu}^{2+}$  to each of these three peptoids results in a decrease in the intensity of the band at about 200 nm and an increase in the intensity of the band at about 220 nm, which is also red-shifted. In the case of **6P6** and **7P6I** this effect is similar to the one observed for the bulky-core segment **4P6**, but although it is more pronounced, these spectra still do not resemble that of a PP-I helix (Figure 7a). Oligomers **7P6** and **7P6I** have the same monomer composition but differ in the number of the *N*smp side-chains near the N-terminus. **7P6** has the two *N*smp monomers near the N-terminus and **7P6I** has only one *N*smp monomer near the N-terminus. However, this small difference is crucial for the PP-I helix formation. In the case of **8P6**,  $\text{Cu}^{2+}$  binding leads to a CD spectrum with two minima at 196 and 222 nm and a maximum at 206 nm (Figure 7a, pink line). This signal closely resembles that of a PP-I helix and is very similar to the spectrum recorded for **7P6** (Figure 7a, blue line). From these results it can be concluded that the combination of a bulky-core motif and at least two *N*smp monomers near the N-terminus, is required for the formation of the PP-I helix upon  $\text{Cu}^{2+}$  coordination. This effect can be assigned to the previously described concept of cooperative folding. Thus, longer peptoid oligomers show more folded secondary structures.<sup>[22]</sup>

It was previously demonstrated that acetylation at the N-terminus of PP-I peptoids can further stabilize their helical structures.<sup>[15,16]</sup> To test this observation in our case, we synthesized oligomers **6P6Ac**, **7P6Ac**, and **8P6Ac** that have the same monomer sequence as **6P6**, **7P6**, and **8P6** respectively but are acetylated. Their CD spectra before and after  $\text{Cu}^{2+}$  addition were recorded and compared with their non-acetylated prototypes. For **6P6Ac** and **7P6Ac** the CD spectra of the free peptoids are very similar in shape and intensity to the spectra of

free **6P6** and **7P6** respectively (Figure S81). For **8P6Ac** the CD spectrum is of similar shape and a somewhat lower intensity compared with **8P6** (Figure S81). These results indicate that the acetylation of the N-terminus has little or no effect on the secondary structure of the free peptoids. The CD spectrum of the  $\text{Cu}^{2+}$  complex of the acetylated **6P6Ac** is also very similar to the spectrum obtained for the  $\text{Cu}^{2+}$  complex of its non-acetylated analogue **6P6** (Figure 7b). In contrast, the CD spectra of the  $\text{Cu}^{2+}$  complexes of the acetylated peptoids **7P6Ac** and **8P6Ac** were found to be very different from that of their non-acetylated prototypes (Figure 7c, 7d). In both cases, the characteristic peaks of the PP-I helix are lost and the CD spectra show typical double minima near 195 and 220 nm, with the larger peak at about 220 nm. In addition, there is a five-fold increase in the intensity of the exciton couplet at the far UV area between 260 and 280 nm. This increase indicates that the acetylation of the N-terminus influenced dramatically the geometry of the  $\text{Cu}^{2+}$  complex. As the higher intensity of the exciton couplet correlates with the smaller dihedral angle of the complex,<sup>[23]</sup> we can assume that the terminal N–H has a significant contribution to the geometry of the copper complex. This contribution was lost upon acetylation leading also to the changes in the PP-I helix. The effect of the acetylation can be assigned to the loss of the hydrogen bonding from the N–H group to the peptoid backbone that decreases the helicity of the peptoid.<sup>[15a]</sup> This results in a less-ordered secondary structure and hence less steric hindrance about the copper center. An alternative explanation would be the intramolecular coordination of the N–H group to the metal center resulting in a tighter helical structure and a more hindered geometry about the copper ion. This coordination would be geometrically possible only for **7P6** and **8P6**, having two *N*<sub>sm</sub> side-chains near the N-terminus (in terms of N–H accessibility to the metal ion), and thus, the effect of N-terminus acetylation is not observed for **6P6** having only one *N*<sub>sm</sub> side chain. However, our UV/Vis titrations and EPR data, which collectively suggest that both HQ ligands are bound to the metal ion in tetragonal coordination geometry, do not support this explanation.

## Conclusions

This work describes the use of metal coordination as a new platform for peptoid folding. Although both the structure and function of peptoids have been extensively explored, and despite the well-established relationships between sequence structure and function in biopolymers, knowledge about these relationships in peptoids is still lacking, limiting their current applications in all fields. Herein we present a systematic study on the secondary structure of peptoid oligomers with mixed chiral aromatic and aliphatic side chains, before and after metal ion addition. We demonstrate that  $\text{Cu}^{2+}$  coordination to a bulky-core peptoid oligomer, bearing two chiral  $\alpha$ -methylbenzyl groups at the 3rd and 4th positions and two HQ ligands at the 2nd and 5th positions, results in the formation of a stable polyproline type-I-like helical secondary structure as evidenced by CD measurements and further supported by EPR spectroscopy. This is in fact the first example of generating a

stable helical secondary structure of a peptoid by means of metal coordination. We show that peptoids, in which chiral bulky side chains do not constitute the majority of their sequences, can fold into pure PP-I-like helices upon metal binding, thus, expanding the diversity of structured peptoid that can be constructed. Based on systematic studies by CD and EPR spectroscopy, we describe, for the first time, the relationship between the peptoids structure and the coordination geometry of the metal centers. We observe the following clear trend within Cu-peptoid complexes: the larger the angle between the two HQ groups is (detected by the lower exciton-coupled CD intensity), the larger is the distortion of the metal center from square planar geometry toward tetrahedral geometry (from EPR data) and the more ordered the peptoid secondary structure (as seen by near-UV signals in the CD spectra). We discovered that in contrast to other peptoid helices, which can be further stabilized by N-terminus acetylation, metallo-peptoid helices are destabilized by this acetylation, hence, the terminal N–H group has a significant role in peptoid folding upon metal coordination. Our findings reveal that the effect of metal binding on the peptoid structure depends both on the peptoid sequence (leading to the initial secondary structure), and on the preferred coordination geometry of the metal ion. These two competing driving forces for peptoid folding can be controlled by sequence design and choice of 1) the number and position of bulky chiral groups, 2) the type of binding ligands and 3) the type of metal ions. We believe that our findings introduce a new platform in peptoid folding, as well as in peptidomimetics structural stabilization, which can impact the design of novel functional biomimetic compounds with diverse sequences.

## Experimental Section

**Materials.** Rink amide resin was purchased from Novabiochem; trifluoroacetic acid (TFA), zinc acetate dehydrate, nickel acetate tetrahydrate, and (S)-(+)-1-methoxy-2-propylamine (*N*<sub>sm</sub>) were purchased from Alfa Aesar; 8-hydroxy-2-quinolinecarbonitrile, (S)-(–)-1- $\alpha$ -methyl-phenylethylamine (*N*<sub>spe</sub>), 4'-chloro-2,2':6,2''-terpyridine, and Manganese acetate tetrahydrate were purchased from Acros; bromoacetic acid, cobalt acetate tetrahydrate, and copper acetate monohydrate were purchased from MERCK; *N,N'*-diisopropylcarbodiimide (DIC), piperidine, benzylamine, acetonitrile, (ACN) and water HPLC grade solvents were purchased from Sigma-Aldrich; dimethylformamide (DMF) and dichloromethane (DCM) solvents were purchased from Bio-Lab Ltd. These reagents and solvents were used without additional purification.

**Instrumentation.** Peptoid oligomers were analyzed by reversed-phase HPLC (analytical C18(2) column, Phenomenex, Luna 5  $\mu\text{m}$ , 100  $\text{\AA}$ , 2.0  $\times$  50 mm) on a Jasco UV-2075 PLUS detector. A linear gradient of 5–95% ACN in water (0.1% TFA) over 10 min was used at a flowrate of 700  $\mu\text{L}/\text{min}$ . The spectrum was recorded at 214 nm. Preparative HPLC was performed using an AXIA Packed C18(2) column (Phenomenex, Luna 15  $\mu\text{m}$ , 100  $\text{\AA}$ , 21.20  $\times$  100 mm). Peaks were eluted with a linear gradient of 5–95% ACN in water (0.1% TFA) over 50 min at a flowrate of 5 mL/min. Mass spectrometry of peptoid oligomers and their metal complexes was performed on a Advion expression CMS mass spectrometer under electrospray ionization (ESI), direct probe CAN/ $\text{H}_2\text{O}$  (95:5), flowrate 0.2 ml/min and

on a Waters LCT Premier mass spectrometer under electrospray ionization (ESI), direct probe CAN/H<sub>2</sub>O (70:30), flowrate 0.3 ml min<sup>-1</sup>. UV measurements were performed using an Agilent Cary 60 UV/Vis spectrophotometer, equipped with a double beam Czerny–Turner monochromator. CD measurements were performed using an Applied Photophysics chirascan circular dichroism spectrometer. EPR spectra were recorded on a Bruker EMX-10/12 X-band ( $\nu=9.4$  GHz) digital EPR Spectrometer. Spectra processing and simulation were performed with Bruker WIN-EPR and SimFonia Software. Data processing was done with KaleidaGraph software.

**Synthesis of the peptoid oligomers.** Solid-phase synthesis of peptoid oligomers was performed in fritted syringes on Rink amide resin using a variation of a previously reported peptoid sub-monomer protocol.<sup>[2]</sup> In a typical oligomer synthesis, 100 mg of resin with a loading level of 0.83 mmol g<sup>-1</sup> was swollen in 4 mL of dichloromethane (DCM) for 40 min. Following swelling, the Fmoc protecting group was removed by treatment with 2 mL of 20% piperidine in dimethylformamide (DMF) for 20 min. After deprotection and after each subsequent synthetic step, the resin was washed three times with 2 mL of DMF, one minute per wash. Peptoid synthesis was carried out with alternating bromoacylation and amine displacement steps. For each bromoacylation step, 20 equiv bromoacetic acid (1.2 M in DMF, 8.5 mL g<sup>-1</sup> resin) and 24 equiv *N,N*-diisopropylcarbodiimide (neat, 2 mL g<sup>-1</sup> resin) were added to the resin, and the mixture was agitated for 20 min. After washing, 20 equiv of the required amine (1.0 M in DMF) were added to the resin and agitated for 20 min. This two-step addition cycle was modified as follows (for 100 mg resin): after incorporation of 8-hydroxy-2-quinolinemethylamine, 0.17 ml of a 1.2 M solution of bromoacetic acid, 0.04 ml of neat *N,N*-diisopropylcarbodiimide (DIC) and 0.29 ml of DMF were added to the resin and mixed at room temperature for 20 minutes.<sup>[18]</sup>

**Acetylation of the peptoid oligomers.** After completion of the peptoid synthesis, 0.17 ml of a 1.2 M solution of acetic acid, 0.04 ml of neat *N,N*-diisopropylcarbodiimide (DIC) and 0.29 ml of DMF were added to the resin and mixed at room temperature for 60 min.

**Cleavage and purification of the peptoid oligomers.** When the desired sequence was achieved, the peptoid products were cleaved from the resin by treatment with 95% trifluoroacetic acid (TFA) in water (50 mL g<sup>-1</sup> resin) for 30 min. After filtration, the cleavage mixture was concentrated by rotary evaporation under reduced pressure for large volumes, or under a stream of nitrogen gas for volumes less than 1 mL. Cleaved samples were then re-suspended in 50% acetonitrile in water and lyophilized to powders. Peptoids were purified by preparative High Performance Liquid Chromatography (HPLC) using a C18 column. Products were detected by UV absorbance at 230 nm during a linear gradient conducted from 5% to 95% solvent B (0.1% TFA in HPLC grade acetonitrile) over solvent A (0.1% TFA in HPLC grade water) in 50 min with a flowrate of 5 mL min<sup>-1</sup>.

**Synthesis of metal complexes for MS analysis.** Samples for MS analysis were prepared shortly before measurements. Typically, a solution of peptoid oligomers (100–200  $\mu$ L 0.5 mM) in MeOH or ACN was treated with metal solution (5 mM in H<sub>2</sub>O or ACN) and the mixture was stirred for 30 min and sent for MS analysis.

**UV/Vis analysis.** Metal binding of peptoid oligomers with metal ions Cu<sup>2+</sup>, Co<sup>2+</sup>, and Zn<sup>2+</sup> was analyzed by titration experiments using UV/Vis measurements. In a typical experiment, 10  $\mu$ L of a peptoid solution (5 mM in methanol) was diluted in 3 ml of 80% aqueous methanol (16.6  $\mu$ M final concentration) and then sequentially titrated with 2  $\mu$ L aliquots of a metal ion (5 mM in H<sub>2</sub>O), in multiple steps, until the binding was completed.

**Circular Dichroism.** Approximately 500  $\mu$ L solutions (5 mM in methanol) of lyophilized peptoids powders were prepared immediately before CD measurements. CD scans were performed at room temperature at concentration of 100  $\mu$ M in solution of 80% aqueous methanol. The spectra were obtained by averaging four scans per sample in a fused quartz cell (path length = 0.1 cm). Scans were performed over the 300 to 190 nm region at a step of 1 nm (scan rate = 1 s step<sup>-1</sup>).

**Synthesis of Cu<sup>2+</sup> complexes for EPR experiments.** Copper complexes for EPR were prepared in methanol (0.5 mL) by addition of 1.1 equiv of copper acetate 10 mM in methanol solution to peptoids **7P1** (4.86 mg, 4.20  $\mu$ mol), **7P2** (4.87 mg, 4.22  $\mu$ mol), **7P3** (4.86 mg, 4.20  $\mu$ mol), **7P4** (4.88 mg, 4.22  $\mu$ mol), **7P5** (5.18 mg, 4.48  $\mu$ mol), **7P6** (4.67 mg, 4.04  $\mu$ mol), **7P7** (4.8 mg, 4.16  $\mu$ mol), and **7P8** (4.01 mg, 3.2  $\mu$ mol). The mixtures were shaken for 1 h. Precipitates were obtained after adding an aqueous solution of NH<sub>4</sub>PF<sub>6</sub> (200  $\mu$ L, 1 M), shaking for 30 min and centrifugation. Precipitates were washed twice with water and lyophilized overnight. **7P1Cu** was obtained in 85% yield (5.27 mg), **7P2Cu**; 91.0% yield (4.63 mg), **7P3Cu**; 80.0% yield (4.87 mg), **7P4Cu**; 81.7% yield (5.21 mg), **7P5Cu**; 93.2% yield (6.30 mg), **7P6Cu**; 77% yield (3.1 mg), **7P7Cu**; 80% yield (3.32 mg), and **7P8Cu**; 82.5% yield (3.46 mg).

## Acknowledgements

The research leading to these results has received funding from the European Union's Seventh Framework Program (FP7/2007-2013) under grant agreement No. 333034-MC-MF STRC AND FCN. The authors thank Mrs. Larisa Panz for her assistance with the various MS measurements and Dr. Boris Tumanskii for his assistance with the EPR measurements. M.B. thanks the Schulich foundation and the Gutwirth foundation for her PhD fellowship.

## Conflict of Interest

The authors declare no conflict of interest.

**Keywords:** helices · metal coordination · peptides · peptoids · secondary structure

- [1] a) W. S. Horne, S. H. Gellman, *Acc. Chem. Res.* **1998**, *31*, 173–180; b) D. J. Hill, M. J. Mio, R. B. Prince, T. S. Hughes, J. S. Moore, *Chem. Rev.* **2001**, *101*, 3893–4012; c) S. Hecht, I. Huc, Eds. *Foldamers: structure, properties, and applications*, **2007**, Wiley-VCH, Weinheim, Germany; d) Seebach, J. Cardiner, *Acc. Chem. Res.* **2008**, *41*, 1366–1375; e) C. Proulx, D. Sabatino, R. Hopewell, J. Spiegel, Y. G. Ramos, W. D. Lubell, *Future Med. Chem.* **2011**, *3*, 1139–1164; f) T. A. Martinek, F. Fulop, *Chem. Soc. Rev.* **2012**, *41*, 687–702; g) G. Maayan, *Eur. J. Org. Chem.* **2009**, 5699–5710; h) G. Maayan, M. Albrecht, Eds. *Metallofoldamers. Supramolecular Architectures from Helicates to Biomimetics*, Wiley, Hoboken, **2013**.
- [2] a) D. S. Ganesh, S. Nabanita, Z. Oyunchimeg, R. N. Zuckermann, P. Saha, *Polym. Bull.* **2017**, *74*, 3455–3466; b) M. Wetzler, A. E. Barron, *Biopolymers* **2011**, *96*, 556–560; c) R. N. Zuckermann, *Biopolymers* **2011**, *96*, 545–555; d) K. E. Drexler, *Biopolymers* **2011**, *96*, 537–707; e) K. J. Prathap, G. Maayan, *Org. Lett.* **2015**, *17*, 2110–2113.
- [3] a) R. J. Simon, R. S. Kania, R. N. Zuckermann, V. D. Huebner, D. A. Jewell, S. Banville, S. Ng, L. Wang, S. Rosenberg, C. K. Marlowe, D. C. Spellmeyer, R. Tan, A. D. Frankel, D. V. Santi, F. E. Cohen, P. A. Bartlett, *Proc. Natl. Acad. Sci. USA* **1992**, *89*, 9367–9371; b) J. A. Patch, K. Kirshenbaum, S. L. Seurnyck, R. N. Zuckermann, A. E. Barron, in *Drug Discovery*; Wiley-VCH

- Weinheim, Germany, **2004**; pp 1–31; c) R. N. Zuckermann, T. Kodadek, *Curr. Opin. Mol. Ther.* **2009**, *11*, 299–307; d) M. T. Dohm, R. Kapoor, A. E. Barron, *Curr. Pharm. Des.* **2011**, *17*, 2732–2747; e) K. H. A. Lau, *Biomat. Sci.* **2014**, *2*, 627–633; f) A. A. Fuller, B. A. Yurash, E. N. Schaumann, F. J. Seidl, *Org. Lett.* **2013**, *15*, 5118–5121.
- [4] R. N. Zuckermann, J. M. Kerr, S. B. W. Kent, W. H. Moos, *J. Am. Chem. Soc.* **1992**, *114*, 10646–10647.
- [5] a) B. C. Lee, T. K. Chu, K. A. Dill, R. N. Zuckermann, *J. Am. Chem. Soc.* **2008**, *130*, 8847–8855; b) N. Maulucci, I. Izzo, G. Bifulco, A. Aliberti, C. De Cola, D. Comegna, C. Gaeta, A. Napolitano, C. Pizza, C. Tedesco, D. Flot, F. De Riccardis, *Chem. Commun.* **2008**, 3927–3929; c) C. De Cola, S. Licen, D. Comegna, E. Cafaro, G. Bifulco, I. Izzo, P. Tecilla, F. De Riccardis, *Org. Biomol. Chem.* **2009**, *7*, 2851–2854; d) G. Della Sala, B. Nardone, F. De Riccardis, I. Izzo, *Org. Biomol. Chem.* **2013**, *11*, 726–731; e) I. Izzo, G. Ianniello, C. De Cola, B. Nardone, L. Erra, G. Vaughan, C. Tedesco, F. De Riccardis, *Org. Lett.* **2013**, *15*, 598–601; f) C. De Cola, G. Fiorillo, A. Meli, S. Aime, E. Gianolio, I. Izzo, F. De Riccardis, *Org. Biomol. Chem.* **2014**, *12*, 424–431; g) C. Tedesco, L. Erra, I. Izzo, F. De Riccardis, *CrystEngComm* **2014**, *16*, 3667–3687; h) T. Zabrodski, M. Baskin, J. K. Prathap, G. Maayan, *Synlett* **2014**, A–F; i) A. S. Knight, E. Y. Zhou, J. G. Pelton, M. B. Francis, *J. Am. Chem. Soc.* **2013**, *135*, 17488–17493; j) A. S. Knight, E. Y. Zhou, M. B. Francis, *Chem. Sci.* **2015**, *6*, 4042–4048; k) K. J. Prathap, G. Maayan, *Chem. Commun.* **2015**, *51*, 11096–11099; l) M. Baskin, G. Maayan, *Chem. Sci.* **2016**, *7*, 2809–2820; m) M. Baskin, L. Panz, G. Maayan, *Chem. Commun.* **2016**, *52*, 10350–10353.
- [6] G. Maayan, M. D. Ward, K. Kirshenbaum, *Chem. Commun.* **2009**, 56–58.
- [7] M. Baskin, G. Maayan, *Biopolymers* **2015**, *104*, 577–584.
- [8] A. S. Knight, E. Y. Zhou, M. B. Francis, R. N. Zuckermann, *Adv. Mater.* **2015**, *27*, 5665–5691.
- [9] C. W. Wu, T. J. Sanborn, R. N. Zuckermann, A. E. Barron, *J. Am. Chem. Soc.* **2001**, *123*, 2958–2963.
- [10] P. Armand, K. Kirshenbaum, A. Falicov, R. L. Dunbrack Jr., K. A. Dill, R. N. Zuckermann, F. E. Cohen, *Fold Des.* **1997**, *2*, 369–375.
- [11] a) G. Maayan, M. D. Ward, K. Kirshenbaum, *Proc. Natl. Acad. Sci. USA* **2009**, *106*, 13679–13684; b) R. Schettini, F. De Riccardis, G. Della Sala, I. Izzo, *J. Org. Chem.* **2016**, *81*, 2494–2505.
- [12] J. Sun, R. N. Zuckermann, *ACS Nano* **2013**, *7*, 4715–4732.
- [13] B. C. Gorske, J. R. Stringer, B. L. Bastian, S. A. Fowler, H. E. Blackwell, *J. Am. Chem. Soc.* **2009**, *131*, 16555–16567.
- [14] C. Caumes, O. Roy, S. Faure, C. Taillefumier, *J. Am. Chem. Soc.* **2012**, *134*, 9553–9556.
- [15] a) J. R. Stringer, J. A. Crapster, I. A. Guzei, H. E. Blackwell, *J. Am. Chem. Soc.* **2011**, *133*, 15559–15567; b) J. A. Crapster, I. A. Guzei, H. E. Blackwell, *Angew. Chem. Int. Ed.* **2013**, *52*, 5079–5084; *Angew. Chem.* **2013**, *125*, 5183–5188.
- [16] a) O. Roy, C. Caumes, Y. Esvan, C. Didierjean, S. Faure, C. Taillefumier, *Org. Lett.* **2013**, *15*, 2246–2249; b) O. Roy, G. Dumonteil, S. Faure, L. Jouffret, A. Kriznik, C. Taillefumier, *J. Am. Chem. Soc.* **2017**, *139*, 13533–13540.
- [17] a) M. J. Kelso, H. N. Hoang, T. G. Appleton, D. P. Fairlie, *J. Am. Chem. Soc.* **2000**, *122*, 10488–10489; b) M. T. Ma, H. N. Hoang, C. G. Scully, T. G. Appleton, D. P. Fairlie, *J. Am. Chem. Soc.* **2009**, *131*, 4505–4512; c) M. R. Ghadiri, C. Choi, *J. Am. Chem. Soc.* **1990**, *112*, 1630–1632; d) M. R. Ghadiri, A. K. Fernholz, *J. Am. Chem. Soc.* **1990**, *112*, 9633–9635; e) F. Ruan, Y. Chen, P. B. Hopkins, *J. Am. Chem. Soc.* **1990**, *112*, 9403–9404; f) P. Rossi, P. Tecilla, L. Baltzer, P. Scrimin, *Chem. Eur. J.* **2004**, *10*, 4163–4170; g) S. R. Gilbertson, G. Chen, M. McLoughlin, *J. Am. Chem. Soc.* **1994**, *116*, 4481–4482; h) S. R. Gilbertson, G. X. Wang, S. Hoge, C. A. Klug, J. Schaefer, *Organometallics* **1996**, *15*, 4678–4680; i) N. Ousaka, N. Tani, R. Sekiya, R. Kuroda, *Chem. Commun.* **2008**, 2894–2896; j) S. Tashiro, K. Matsuoka, A. Minoda, M. Shionoya, *Angew. Chem. Int. Ed.* **2012**, *51*, 13123–13127; *Angew. Chem.* **2012**, *124*, 13300–13304; k) S. J. Smith, R. J. Radford, R. H. Subramanian, B. R. Barnett, J. S. Figueroa, F. A. Tezcan, *Chem. Sci.* **2016**, *7*, 5453–5461; l) S. J. Smith, K. Du, R. J. Radford, F. A. Tezcan, *Chem. Sci.* **2013**, *4*, 3740–3747.
- [18] G. Maayan, B. Yoo, K. Kirshenbaum, *Tetrahedron Lett* **2008**, *49*, 335–338.
- [19] a) S. F. Sousa, A. B. Lopes, P. A. Fernandes, M. J. Ramos, *Dalton Trans.* **2009**, *38*, 7946–7956; b) C. Andreini, I. Bertini, G. Cavallaro, *PLoS One* **2011**, *6*, e26325; c) L. Mishra, K. Bindu, S. Bhattacharya, *Spectrochim. Acta* **2005**, *61*, 807–813.
- [20] H. M. Shin, C. M. Kang, M. H. Yoon, J. Seo, *Chem. Commun.* **2014**, *50*, 4465–4468.
- [21] F. Rabanal, M. D. Ludevid, M. Pons, E. Giralt, *Biopolymers* **1993**, *33*, 1019–1028.
- [22] C. W. Wu, K. Kirshenbaum, T. J. Sanborn, J. A. Patch, K. Huang, K. A. Dill, R. N. Zuckermann, A. E. Barron, *J. Am. Chem. Soc.* **2003**, *125*, 13525–13530.
- [23] N. Berova, L. Di Bari, G. Pescitelli, *Chem Soc Rev* **2007**, *36*, 914–931.
- [24] a) G. J. Palenik, *Acta Crystallogr.* **1964**, *17*, 687; b) R. C. Hoy, R. H. Morriss, *Acta Crystallogr.* **1967**, *22*, 476–482.
- [25] U. Sakaguchi, A. W. Addison, *Dalton Trans.* **1979**, 600–608.
- [26] H. R. Gersmann, J. D. Swalen, *J. Chem. Phys.* **1962**, *36*, 3221–3233.

Manuscript received: September 22, 2017

Accepted manuscript online: October 20, 2017

Version of record online: December 4, 2017